JOURNAL OF FORENSIC SCIENCES

J Forensic Sci, November 2011, Vol. 56, No. 6
doi: 10.1111/j.1556-4029.2011.01870.x
Available online at: onlinelibrary.wiley.com

TECHNICAL NOTE

CRIMINALISTICS

Kelly M. Elkins,[1] *Ph.D.*

Rapid Presumptive ''Fingerprinting'' of Body Fluids and Materials by ATR FT-IR Spectroscopy*,†

ABSTRACT: Human body fluids and materials were evaluated using attenuated total reflectance Fourier transform infrared spectroscopy. Purified proteins, cosmetics, and foodstuffs were also assayed with the method. The results of this study show that the sampled fluids and materials vary in the fingerprint region and locations of the amide I peaks because of the secondary structure of the composite proteins although the C=O stretch is always present. The distinct 1016 cm^{-1} peak serves as a signature for semen. The lipid-containing materials (e.g., fingerprints, earwax, tears, and skin) can also be easily separated from the aqueous materials because of the strong CH_3 asymmetric stretch of the former. Blood–saliva and blood–urine mixtures were also successfully differentiated using combinations of peaks. Crime scene investigators employing rapid, portable, or handheld infrared spectroscopic instruments may be able to reduce their need for invasive, destructive, and consumptive presumptive test reagents in evaluating trace evidence.

KEYWORDS: forensic science, Fourier transform infrared (FTIR) spectroscopy, spectroscopic imaging, trace evidence, blood, saliva, hair, semen, urine, feces

The forensics field continues to need presumptive tests for the routine qualitative identification of encountered substances. Presumptive tests indicate the presence of a substance or class of substances but not the quantity of the material or its overall quality for use in subsequent confirmatory tests. Many techniques have been established for presumptive forensic evaluation, but as new instrumentation and techniques are developed, laboratories must evaluate whether the methods they currently employ remain the most cost and time efficient as well as the least invasive and destructive, yet provide reliable and validated methods for use by our criminal justice system. Since 1999, scientists have been working to develop handheld instrumentation for the crime scene (1). This report details the use of a chemical analysis instrument for onsite preliminary analysis in investigations for biological samples including blood, earwax, feces, fingernails, fingerprints, hair, nasal mucus, vaginal mucus, saliva, semen, and urine commonly recovered by crime scene investigators at crime scenes in the presumptive testing and partitioning of these samples from look-alike samples for proper collection and indication of confirmation analyses. Without a reliable and quick presumptive test, evidence may easily be missed, be misidentified, and risk receiving improper packaging in the crime scene setting or become compromised prior to confirmatory testing. Many agencies use the portable UV light or the alternative light source as preliminary tests for finding and presumptively identifying body fluids at the scene prior to further confirmatory testing in the laboratory. Virkler and Lednev recently published an excellent review of presumptive and confirmatory tests for blood, saliva, semen, vaginal fluid, urine, and feces (2), but there is no previous report of the use of attenuated total reflectance Fourier transform infrared (ATR FT-IR) spectroscopy for this purpose yet even smaller crime laboratories are equipped with this instrumentation. The published and established techniques have weaknesses in terms of time (e.g., thin layer chromatography, high performance liquid chromatography, electrophoresis) (2), destructiveness, and carcinogenicity (e.g., chemical reagents) (2–8), specificity (e.g., UV–Vis, microscopy, and chemical reagents) (2–9), and cost (e.g., antibody tests and SEM/EDX) (2–4,6,10–17). ATR FT-IR spectroscopy has significant advantages in that there are no consumable costs or chemical reagents, scan time is very fast, and it is specific in differentiating biological materials. There is no published presumptive forensic test for breast milk, tears, or nasal mucus.

Infrared (IR) spectroscopy is an accepted method used to evaluate evidence such as alcohol, drugs and other white powders and derivatives, inks, fibers, anodization treatment and surface oxides, paints, and primers (http://www.sigmaaldrich.com/labware/products/sensir-atr-library.html; http://riodb01.ibase.aist.go.jp/sdbs/cgi-bin/direct_frame_top.cgi) (18–20). IR spectroscopy is also used for the identification of nerve and blister agents, industrial chemicals, weapons of mass destruction, chemical precursors, common household and laboratory chemicals, solvents, explosives, and propellants (http://www.sigmaaldrich.com/labware/products/sensir-atr-library.html; http://riodb01.ibase.aist.go.jp/sdbs/cgi-bin/direct_frame_top.cgi) (21–23). In other fields, IR spectroscopy has been used to examine salivary proteins (24–26), urine (27–29), fingerprints (30), blood (31–33), hair (34–36), cerumen (37), breast milk (38,39), vaginal mucus (40), feces (41), tears (42,43), and

[1]Department of Chemistry, Criminalistics Program, Metropolitan State College of Denver, PO Box 173362, Campus Box 52, Denver, CO 80217-3362.

*Presented as a poster presentation at the 61st American Academy of Forensic Sciences Annual Meeting, February 16–21, 2009, in Denver, CO.

†Funding and support provided by the Metro State Chemistry Department.

Received 23 Dec. 2009; and in revised form 20 Oct. 2010; accepted 23 Oct. 2010.

semen (44) biological samples but its use in evaluating and differentiating forensic samples has not been reported. ATR FT-IR spectroscopy is a technique that requires no sample preparation, little technical expertise to run the instrument and requires only two drops (10–20 μL) of liquid or a small amount of solid sample (enough to cover the diamond surface). ATR FT-IR spectroscopy is noninvasive and nondestructive as well as rapid in terms of data acquisition. Depending on the desired spectral resolution and how many spectra are to be averaged, ATR FT-IR spectroscopy requires approximately 10 sec (four scans) to 5 min (128 scans). This report is a conceptual demonstration of direct ATR FT-IR spectroscopic methods and second-derivative analysis for the use as a presumptive test of biological evidence at a crime scene or in the laboratory. It has already been shown that FT-IR spectroscopy can be applied to a variety of biological samples. This work will demonstrate that ATR FT-IR spectroscopy is a quick, nondestructive method for differentiating between different types of biological samples, including blood, earwax, feces, fingernails, fingerprints, hair, nasal mucus, vaginal mucus, saliva, tears, and urine. Initial studies have also been performed on mixtures of stains and biological samples exposed to heat. Finally, to the author's knowledge, this is the first report of the use of IR spectroscopy to evaluate tears and nasal mucus.

Materials and Methods

Spectra of samples of human body fluids and solid materials including blood, earwax, feces, fingernails, fingerprints, hair, nasal mucus, vaginal mucus, saliva, tears, and urine were collected without preprocessing by placing the simulated questioned sample directly on the cleaned diamond crystal surface as a native liquid or solid. Semen standard was purchased (Lot #705; Seratec, Richmond, CA) and thawed before using in the liquid form as above. For comparison, simulated forensic evidence samples of the above human body fluids and materials and comparative cosmetic and foodstuff materials including barbeque sauce, lotions, Italian and Catalina dressings, mayonnaise, Vaseline, chocolate, coffee, wine, cream cheese, ketchup, lipstick, and yogurt were also evaluated on a square pieces of a new white 100% cotton T-shirt (Hanes) on the diamond crystal surface. Other simulated samples of saliva and blood were evaluated on white copier paper. Fresh body fluid samples were tested and retested for a total of at least three times over a 2-year period. The locations of the samples were known before the spectra were collected. Samples were obtained from a healthy, anonymous donor in accordance with Metro State Human Review Board, NIJ privacy guidelines, and Helsinki Convention (45). Lyophilized bovine hemoglobin, bovine albumin, α-amylase from porcine pancreas were purchased from Sigma (St. Louis, MO) and used as standard protein samples to compare to the simulated forensic evidence samples known to contain these proteins.

IR spectra were collected on a Thermo Electron Corporation Nicolet 380 (Waltham, MA) using an ATR FT-IR spectrophotometer equipped with the OMNIC 2005 software version 7.2a (Thermo Electron Corporation, Madison, WI). Spectra were recorded from 4000 to 400 cm^{-1} with a resolution of 4 (a data spacing of 1.929 cm^{-1}) or a resolution of 8 (a data spacing of 0.964 cm^{-1}), signal averaged over 128 scans, and data saved as a .CSV text file that was imported into Microsoft Excel for further imaging and second-derivative analysis. The spectrometer was blanked with air at room temperature for the raw samples or with a clean piece of the white cotton T-shirt or white copier paper for the simulated forensic samples, respectively, and cleaned with alcohol wipes between samples.

Citrated sheep blood purchased from Colorado Serum Company (Denver, CO) was used for comparison with the human blood samples and for the temperature experiments. For the temperature study, prior to spectroscopy, the blood, saliva, and 1:1 mixed blood/saliva simulated evidence samples were dried in clean 10-mL beakers at 21°C (room temperature), 40°C (warm summer day temperature), and 110–120°C (as indicated) (hot vehicle or low arson temperature), which were subsequently scraped with a metal spatula to produce a fine powder. A small amount of the solid sample was transferred using a new, cut-off plastic pipette and placed on the instrument sufficient to completely cover the diamond crystal surface and spectra recorded as above.

Results and Discussion

ATR FT-IR spectra were collected for human blood, earwax (cerumen), feces, fingernails, fingerprints, hair, nasal mucus, vaginal mucus, saliva, tears, and urine body fluid samples and materials. All of the biological materials contain protein but are heterogeneous in nature and contain DNA, RNA, saccharides, lipids, and small molecules. Band assignments were performed using standard correlation charts and one compiled for proteins and lipids (Table 1).

Representative ATR FT-IR spectra (percent transmittance [%T] vs. wavenumber) for sheep blood (line A) and three human blood samples (lines B–D) are shown in Fig. 1. The samples are reproducible: The peaks are in the same positions and relative stretching patterns for the three human blood samples. Blood is a highly heterogeneous material that contains hemoglobin (2DN1.pdb), fibrinogen, albumin (1BMO.pdb), immunoglobulins, red blood cells, white blood cells, platelets, plasma, electrolytes, iodine, sulfate, and glucose and other sugars (2). The samples were collected in their natural form (e.g., liquid) using an air blank (Fig. 1 lines A,B) or dried on a new, white T-shirt (Fig. 1 lines C,D). The visualization of the spectral bands was improved by analyzing the raw spectral data in a graphing program (Microsoft Excel). Figure 1 demonstrates the

TABLE 1—*Attenuated total reflectance Fourier transform infrared spectroscopy correlation chart for proteins (25,27,39).*

IR spectoscopic region (cm^{-1})	Secondary structure
200	Skeletal torsion
537–606	Out-of-plane C=O bending
640–800	Out-of-plane NH bending
725–767	OCN bending + others
1016	Asymmetric O–C–C stretch ester
1229–1301	Amide III (CN stretch, NH bend, and CO in-plane bend)
1400	Symmetric CH_3
1450	Asymmetric CH_3
1456	CH_2 scissors
1480–1575	Amide II (CN stretch and NH in-plane bend)
1600–1690	Amide I (C=O stretch)
1624–1642	β sheet
1640–1648	Random coil
1650–1658	α helix
1660–1665	3–10 helix, π helix, type III turn
1665–1685	Turns
>1680	β sheet & β turn
1744	Saturated ester
1951	Fe^{2+}
2122	Fe^{3+}
2550–2590	Cys S–H stretch
2856	Methylene C–H stretch
2920	Methyl C–H stretch
3275	O–H stretch

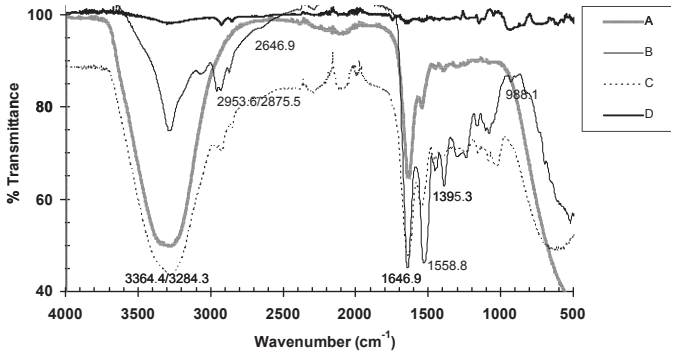

FIG. 1—*Comparison of representative attenuated total reflectance Fourier transform infrared spectra (%T vs. wavenumber from 4000 to 500 cm^{-1}) of four blood samples: (A) sheep blood, (B) human blood (liquid), (C) human blood (dried on white T-shirt), and (D) human blood (dried on white T-shirt).*

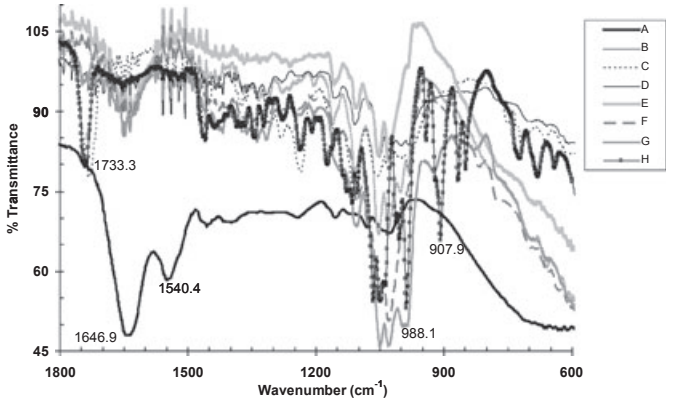

FIG. 2—*Comparison of representative attenuated total reflectance Fourier transform infrared spectra (%T vs. wavenumber from 1800 to 600 cm^{-1}) of simulated forensic blood and comparative cosmetic and foodstuffs samples on a new, white T-shirt: (A) human blood, (B) peppermint lotion, (C) lipstick, (D) wine, (E) ketchup, (F) BBQ sauce, (G) Catalina dressing, and (H) chocolate.*

major peaks for blood as well as the additional fine structure in and around the peaks and the stretching intensity or broadness in part owing to concentration effects but also owing to the differing constituent molecules. The contribution of the proteins in blood predominates especially peaks of the amide I region (1700–1600 cm^{-1}) and water and hydroxyls in the O–H stretch (3500–3200 cm^{-1}) region. The major peaks are located at 3346.4 cm^{-1} (O–H stretch), 3284.3 cm^{-1} (H-bonded O–H stretch), 1646.9 cm^{-1} (amide I random coil), and 1558.8 cm^{-1} (amines bend). Medium to weak peaks are located at 2953.6 cm^{-1} (terminal methyl C–H stretch), 2875.5 cm^{-1} (CH_2 symmetric stretch), 2646.9 cm^{-1} (S–H stretch), 1457.1 cm^{-1} (CH_2 scissors), 1395.3 cm^{-1} (symmetric CH_3), 1244.9 cm^{-1} (amide III), 1162.9 cm^{-1} (C–O, lipid ester), and 981.2 cm^{-1} (C–N–C). The blood protein hemoglobin is α-helical (2DN1.pdb), contains an iron cofactor and its heme coenzyme, and serves as a carrier of oxygen and carbon dioxide; the bonds between the protein and ligands can be identified using FT-IR spectroscopy (32). The weak band at 1112.8 cm^{-1} may be attributed to Fe^{2+} bound to O_2; this was observed at 1107 cm^{-1} in a published study (32). A complete listing of all bands is found in Table 1.

Figures 2–6 contain representative spectra collected on body fluids and compared with common foodstuffs and cosmetic samples. For these spectra, samples were applied individually to squares of a new, white T-shirt to create simulated forensic samples. Figure 2 shows the results of experiments with human blood, peppermint lotion, lipstick, wine, ketchup, BBQ sauce, Catalina dressing, and chocolate (Fig. 2 lines A–H, respectively). Blood (A) can easily be distinguished from the other materials by its large bands at 1646.9 and 1504.4 cm^{-1}, among others. For example, the 1733.3 and 907.9 cm^{-1} bands differentiate chocolate (H) and the three sharp 1500 cm^{-1} region bands (1558.8, 1540.3, and 1507 cm^{-1}) and 988.1 cm^{-1} peak differentiate Catalina dressing (G) (as well as the 2927.6 cm^{-1} CH_3 asymmetric stretch, not shown). Figure 2 shows that blood can be clearly differentiated from the comparative cosmetics and foodstuffs in the amide I region and the fingerprint region.

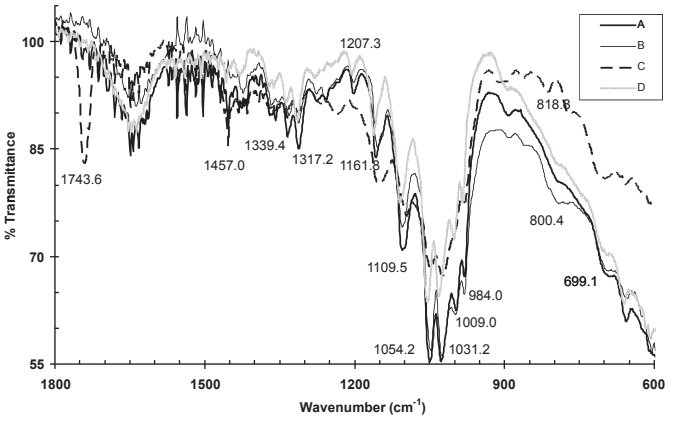

FIG. 3—*Comparison of representative attenuated total reflectance Fourier transform infrared spectra (%T vs. wavenumber from 1800 to 600 cm^{-1}) of simulated forensic urine and comparative cosmetic and foodstuffs samples on a new, white T-shirt: (A) human urine, (B) apple juice, (C) Italian Dressing, and (D) coffee.*

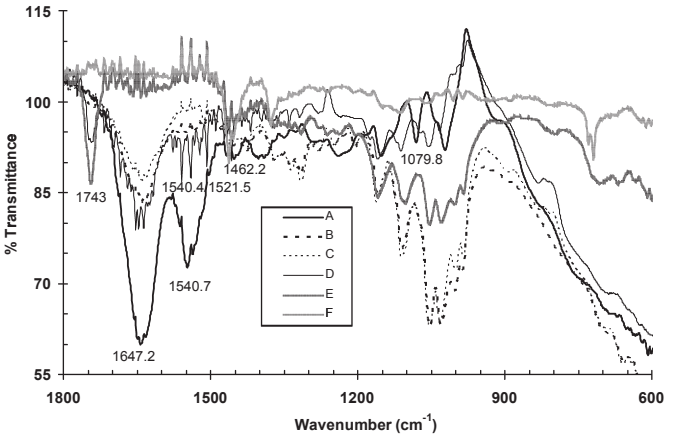

FIG. 4—*Comparison of representative attenuated total reflectance Fourier transform infrared spectra (%T vs. wavenumber from 1800 to 600 cm^{-1}) of simulated forensic vaginal mucus and comparative cosmetic and foodstuffs samples on a new, white T-shirt: (A) human vaginal mucus, (B) yogurt, (C) Oil of Olay, (D) cream cheese, (E) mayonnaise, and (F) Vaseline.*

Figure 3 shows the representative ATR FT-IR spectra of urine (A) as compared to similar-looking materials including apple juice (B), Italian dressing (C), and coffee (D). Urine contains nitrogenous waste including urea and uric acid in addition to B-vitamins, electrolytes (including sodium, chloride and potassium ions, sulfate, and calcium phosphate), trace amounts of protein (including amylase, hemoglobin, myoglobin, and Tamm-Horsfall glycoprotein),

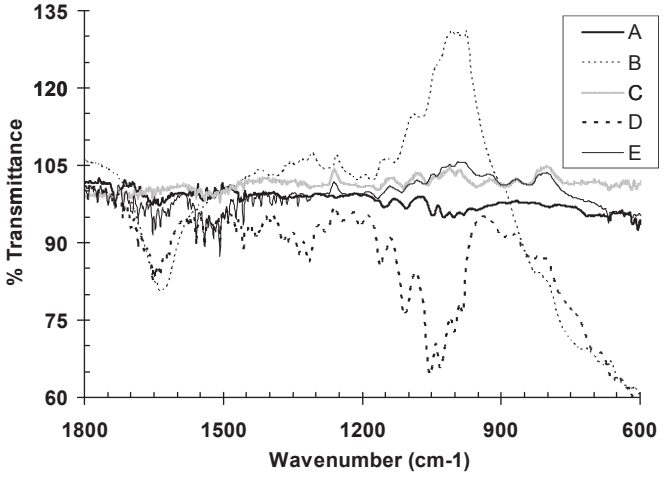

FIG. 5—*Comparison of representative attenuated total reflectance Fourier transform infrared spectra (%T vs. wavenumber from 1800 to 600 cm^{-1}) of human simulated forensic body fluids and materials samples on a new, white T-shirt: (A) tears, (B) semen, (C) feces, (D) nasal mucus, and (E) fingernails.*

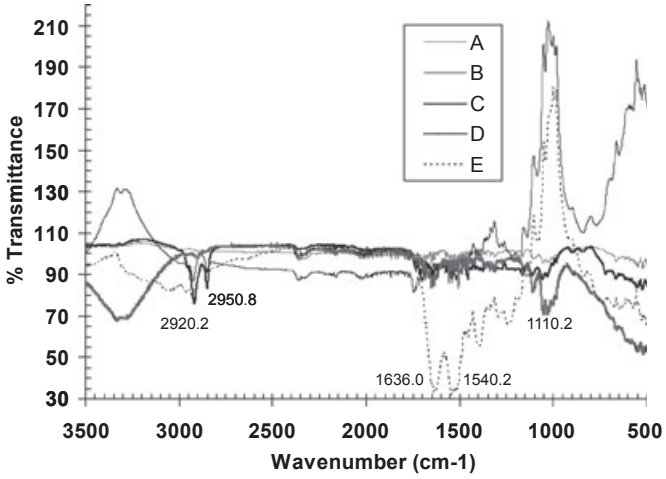

FIG. 6—*Comparison of representative attenuated total reflectance Fourier transform infrared spectra (%T vs. wavenumber from 3500 to 500 cm^{-1}) of human simulated forensic body fluids and materials samples on a new, white T-shirt: (A) hair, (B) fingerprints, (C) cerumen, (D) saliva, and (E) skin.*

and organic compounds (including bilirubin, creatinine, citric acid, cortisol, dopamine, epinephrine, glucose, homovanillic acid, ketones, porphyrins, red blood cells, and vanillylmandelic acid), and it has been evaluated by IR spectroscopy in previous studies (2,46). The major vibrational bands for urine include the following: O–H stretching: 3335.5 cm^{-1}; H-bonded O–H stretching: 3301.7 cm^{-1}; CH_3 asymmetric stretch: 2918.9 cm^{-1}; CH_2 symmetric stretch: 2875.5 cm^{-1}; amide β turn: 1669.5 cm^{-1}; amide I α helix: 1653.0 cm^{-1}; amide I random coil: 1646.9 cm^{-1}; amide I band β sheet: 1636 cm^{-1}; amide II band (C–N stretch and N–H in-plane bend): 1540.3 cm^{-1}; asymmetric CH_3 bending: 1436.8 cm^{-1}; CH_2 scissors: 1457.0 cm^{-1}; symmetric CH_3 bending: 1398.2 cm^{-1}; amide III (C–N stretch, N–H bend, and C=O in-plane bend): 1282.5 cm^{-1}; C–O, lipid ester: 1161.8 cm^{-1}; C–O–P–O–C diester stretch: 1054.2 cm^{-1}; asymmetric O–C–C stretch ester: 1031.2 cm^{-1}; C–N–C: 1000.9 cm^{-1}; and OH carboxylic acid: 984.0 cm^{-1}. An earlier report using near IR spectroscopy to quantify compounds in urine samples focused on the bands at 2152 and 2195 cm^{-1} (47). These peaks are observed (2157.1 and 2197.6 cm^{-1}) but are very weak as compared with other spectral regions.

Subtle differences for differentiating these samples can be observed in the fingerprint region shown. For example, peaks at 1753.6 and 818.8 cm^{-1} are observed with the Italian dressing (D) but not urine. The apple juice (B) has a stronger 800.4 cm^{-1} peak than the urine sample. The coffee (D) sample lacks the 699.1 cm^{-1} peak observed in the other samples.

Figure 4 shows the representative ATR FT-IR spectra of vaginal mucus (A) as compared to appropriate comparative materials including yogurt (B), Oil of Olay (C), cream cheese (D), mayonnaise (E), and Vaseline (F). Vaginal secretions are composed of bacteria and fungi as well as prostaglandins, immunoglobulins, glucose, galactose, fucose, chloride, *N*-acetylglucosamine, *N*-acetylgalactosamine, sialic acid, acid phosphatase, lactic acid, citric acid, acetic acid, urea, a peptidase, epithelial cells, pyridine, squalene, and a L-fucosidase protein (2). The major vibrational bands for vaginal mucus include the following: H-bonded O–H stretching: 3188.9 cm^{-1}; C=C CH stretch: 3079.9 cm^{-1}; terminal methyl C–H stretch: 2936.2 cm^{-1}; CH_2 symmetric stretch: 2859.1 cm^{-1}; S–H stretch: 2654.7 cm^{-1}; amide I random coil: 1647.2 cm^{-1}; amide I band β sheet: 1643.3 cm^{-1}; amide II band (C–N stretch and N–H in-plane bend): 1540.7 cm^{-1}; CH_2 scissors: 1457.1 cm^{-1}; symmetric CH_3 bending: 1395.4 cm^{-1}; asymmetric stretch of PO_2^- groups: 1289.2 cm^{-1}; amide III (C–N stretch, N–H bend, and C=O in-plane bend): 1238.4 cm^{-1}; C–O, lipid ester: 1150.4 cm^{-1}; C–OH glycoprotein: 1079.8 cm^{-1}; asymmetric O–C–C stretch ester: 1018.3 cm^{-1}; and OH carboxylic acid: 921.6 cm^{-1}. The peaks appear to be at the same locations as those IR spectra reported by another group (40).

The following peaks are unique to the comparative samples as compared to the vaginal mucus: yogurt (B): peaks at 1052.0 and 1030.4 cm^{-1}; Oil of Olay (C): peaks at 1053.3 and 1031.6 cm^{-1}; cream cheese (D): double peaks at 1558.8 and 1540.4 cm^{-1} and a peak at 1743.4 cm^{-1}; mayonnaise (E): a peak at 1743.4 cm^{-1}; and Vaseline (F): peak at 719.3 cm^{-1}.

Figure 5 shows the representative ATR FT IR spectra of human body fluids and materials including tears (A), semen (B), feces (C), nasal mucus (D), and fingernails (E). Tears consist of proteins including sIgA, lactoferrin, tear-specific pre-albumin, serum albumin, protein G, and the antimicrobial agent lysozyme, in addition to lipids (e.g., wax, cholesterol, and phospholipids) and mucins (42). Semen contains a heterogeneous list of compounds and ions including acid phosphatase, prostate-specific antigen, citric acid, inositol, calcium, zinc, magnesium, fructose, ascorbic acid, prostaglandins, L-carnitine, fructose, neutral α-glucosidase, choline, spermine, seminogelin, urea, ascorbic acid, immunoglobulins, sperm cells, and albumin, which makes up about one-third of the protein content (which is higher than that of plasma) (2,48). Fecal matter consists of colon cells, lipids, and indigestible polysaccharides as well as other metabolic wastes. Nasal mucus contains proteins and glycoprotein and bacterial cells (49,50). A comparison of the spectra and peaks listed in Table 1 indicate that the *c*. 3300 cm^{-1} peak is present for all of these materials except feces. Tears, semen, and nasal mucus do not exhibit a *c*. 3000 cm^{-1} peak. The *c*. 2900 cm^{-1} peak is observed in the spectra of tears and mucus. The 2856 cm^{-1} peak is observed from the tears, feces, and fingernails. The C=O/ester peak is observed in the spectra of the nasal mucus, tears, and feces, and the C=O COOH peak is observed in the nasal mucus. These materials, with the exception of semen, all exhibit the amide I β turn, amide I α-helix, amines bend, and amide II

band. The conjugated dienes peak is found in the feces and nasal mucus spectra. The amide I region random coil is exhibited by the nasal mucus, tears, and fingernails. The CH_2 scissors stretch is exhibited by the nasal mucus, feces, and fingernails. The CH in-plane bend is exhibited by all of these spectra except the semen and fingernails, and the amide III stretch is not found in the semen and nasal mucus spectra. All of the materials exhibit the amide I β sheet and the OH carboxylic acid stretches. The largest differences are in the fingerprint region shown in the figure. In other studies, semen was found to produce FT-IR spectroscopic bands at 1087, 966, 1657, 1547, 1450, 1400, 1236, 1087, and 1740 cm^{-1} (44) and tears were found to have bands at 1242, 1546, 1735, and 2852 cm^{-1} (43). Feces were found to exhibit bands at 2310, 2270, 1818, 1778, 1734, and 1187 nm in absorbance spectra (41).

Figure 6 shows the representative ATR FT-IR spectra of human body fluids and materials including hair (A), fingerprints (B), cerumen (C), saliva (D), and skin (E). Hair is composed of the proteins collagen (a coiled coil) and keratin, which has a β turn secondary structure with small amounts of β sheet (51). Earwax (cerumen) consists of lipids including long-chain saturated and unsaturated fatty acids, alcohols, wax esters and cholesterol, squalene, and triglycerides; sugars including galactosamine and galactose; and protein material including amino acids, keratin, and desquamated keratinocytes (52,53). Saliva is a very dilute solution (99% water) but contains a complex mixture of aqueous proteins including aquaporin, peroxidases, immunoglobulins, lysozyme, the glycoprotein osteonectin, an acidic proline-rich protein, histidine-rich proteins, such as histatins, cystatins, statherin, mucins, partially degraded proteins, and the α-amylase enzyme for digestion of sugars as well as buccal epithelial cells, bacteria, sodium, potassium, calcium, magnesium, phosphate, thiocyanate and bicarbonate salts, urea and ammonia, glucose sugars, and the cortisol lipid (2,54). The saliva protein α-amylase consists of α and β structures as well as loops and turns (1SMD.pdb).

A comparison of the spectra in Fig. 6 and the peaks listed in Table 1 indicate that the *c*. 3300 cm^{-1} peak is present for all of these materials except cerumen. Cerumen, fingerprints, and saliva do not exhibit a *c*. 3000 cm^{-1} peak. All of these materials exhibit the *c*. 2900 cm^{-1} peak. The 2856 cm^{-1} peak is observed from the cerumen and skin. The C=O/ester peak is observed in the spectra of the fingerprints and cerumen, and the C=O carboxylic acid peak is observed in the cerumen spectrum. These materials, with the exception of saliva, all exhibit the amide I β turn, while only the skin does not exhibit the amide I α-helix. The fingerprints and cerumen spectra exhibit the amide I random coil. All of the materials except the fingerprints exhibit the amide I β sheet. All of the spectra except for that of skin exhibit the amines bend. All of the materials shown in this figure exhibit the amide II band, but the conjugated dienes peak is not found in the materials shown here. The CH_2 scissors stretch is exhibited by the fingerprints, cerumen, and hair. The CH in-plane bend is exhibited by all the hair and fingerprints, and the amide III stretch is not found in the cerumen and saliva spectra. The OH carboxylic acid stretches are not seen in the saliva and skin spectra but are observed in the other spectra.

The largest differences are in the fingerprint region as shown in the figure. In a previous study, a peak at 1044 cm^{-1} was found to be most useful for detecting levels of oxidation of the hair (35) and keratin was found to have peaks at 1650, 1620, and *c*. 1550 cm^{-1} (36). The lowest peak intensity can be attributed to short peptides, which explains the weak intensity of fingerprints (27). Previously, fingerprints were found to exhibit the following IR spectroscopic peaks: 2920, 2856, 1744, 1656, 1552, 1456, 1248, and 1016 cm^{-1}, congruent with the results shown here (30).

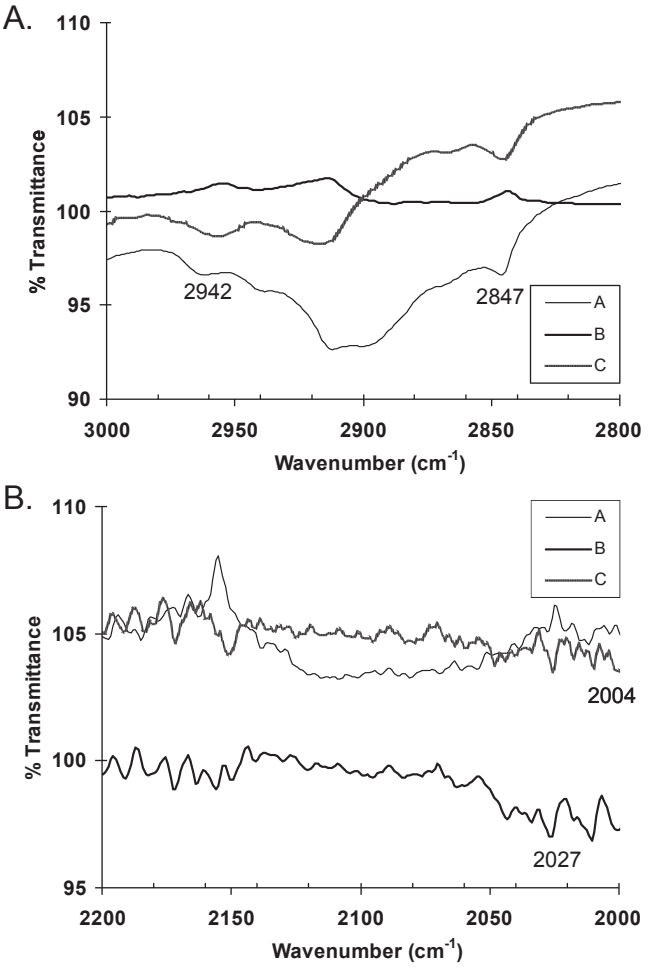

FIG. 7—*Comparison of representative attenuated total reflectance Fourier transform infrared spectra (%T vs. wavenumber): (A) from 3000 to 2800 cm^{-1} and (B) 2200–2000 cm^{-1} for three human simulated forensic samples on a new, white T-shirt: (A) urine, (B) blood, and (C) human urine added to human blood (dried on white T-shirt).*

Figure 7*A,B* show the comparison of representative ATR FT-IR spectra of three samples on a new, white T-shirt including urine (A), blood (B), and human urine added to human blood (C) for %T versus wavenumber from 3000 to 2800 cm^{-1} and 2200 to 2000 cm^{-1}, respectively. The blood/urine mixture spectrum exhibits approximately averaged features observed in the blood and urine samples alone. Figure 7*A* shows that urine (A) has weak unique peaks at 2942 and 2847 cm^{-1}. The mixture (C) exhibits both peaks. The peaks in the urine (A) spectra are out of phase with those of blood (B) from *c*. 2350 to 2300 cm^{-1} (data not shown). The mixture (C) exhibits the blood-like peaks in this region. Figure 7*B* shows that blood (B) has a unique weak peak at 2027 cm^{-1}, which the mixture (C) also exhibits. Urine (A) has a unique weak peak at 2004 cm^{-1}, which the mixture (C) also exhibits.

Additional experiments were performed on sheep's blood and human saliva to determine the effects of heat on the ATR FT-IR spectra. Figure 8 shows the results of this study: Fig. 8*A* contains the original ATR FT-IR spectra plotted as %T versus wavenumber from 4000 to 400 cm^{-1} and Fig. 8*B* contains the second derivative of %T plots of these spectra in the 1800–1600 cm^{-1} region for the heated samples (dried at room temperature, 21°C, and 120°C). There were no discernable spectral differences between human

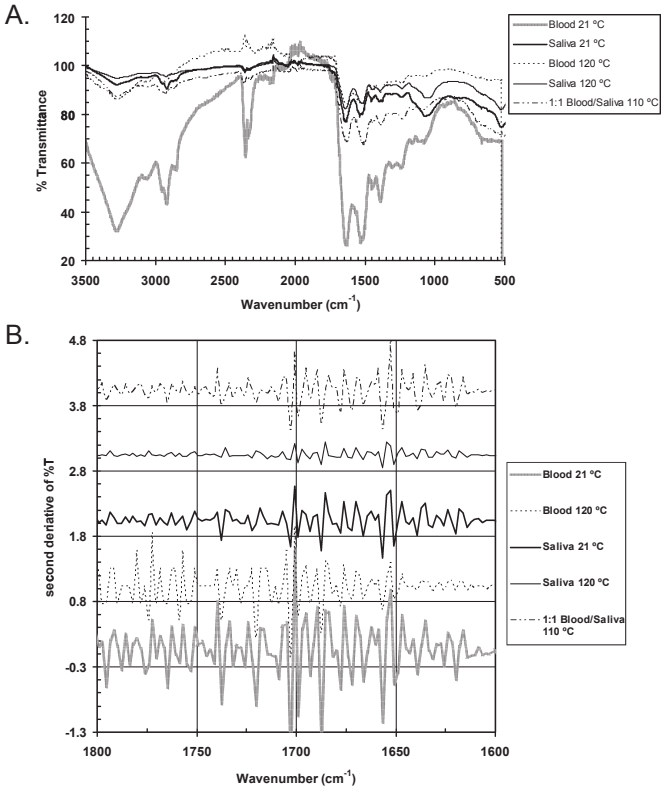

FIG. 8—*Attenuated total reflectance Fourier transform infrared spectra of blood and saliva dried at room temperature (21°C) and in an oven (120°C) and 1:1 mixture of blood and saliva dried in an oven (110°C): (A) raw %T spectra from 3500 to 500 cm^{-1}, (B) second derivative of %T plots in the amide I region from 1800 to 1600 cm^{-1}.*

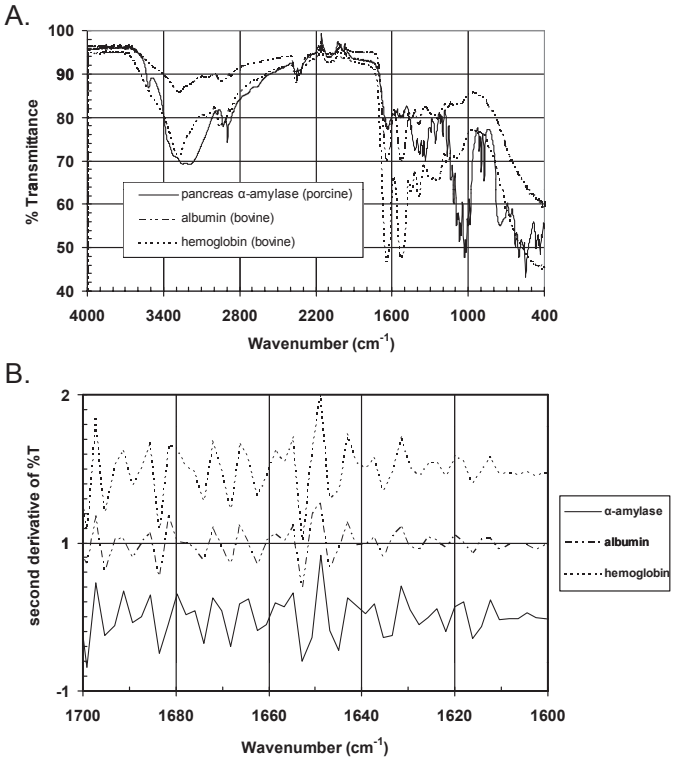

FIG. 9—*Attenuated total reflectance Fourier transform infrared spectra of protein standards α-amylase, hemoglobin, and albumin: (A) raw %T spectra from 4000 to 400 cm^{-1}, (B) second derivative of %T plots in the amide I region from 1700 to 1600 cm^{-1}.*

(previous figures) and sheep's blood. Upon comparison of the spectra of blood or saliva dried at room temperature or at a high temperature, it is evident that the spectra have not been altered by the heat although the intensity of the spectra has been diminished by the heating, most likely owing to protein degradation. By comparing the raw data and second-derivative plots, similarities and differences can clearly be observed in this region as the second-derivative plots more clearly show the weak peaks. High sensitivity to small variations in protein secondary structure (Table 1), molecular geometry, and hydrogen bonding makes the amide I region uniquely useful for analyzing otherwise similar protein structures in the second-derivative plot. Primary differences between the blood and saliva second-derivative plots are observed at 1649, 1652, 1654, 1670, 1684, and 1686 cm^{-1}. The 1:1 mixture of blood/saliva by volume has unique features (e.g., 1315, 1175, and 669 cm^{-1} peaks) derived from the blood, but not saliva, spectra. The second-derivative spectrum for the mixture also differs from that observed in either the blood or the saliva spectra taken alone; the peak shape differences are especially noticeable in the second-derivative plot. The peaks in the blood samples are also more intense than those from saliva. In conclusion, although the ATR FT-IR spectra of blood and saliva dried at the two temperatures (21°C and 120°C) do not differ in the frequencies of the exhibited peaks, these spectra can reveal a complex mixture as in Fig. 7. The mixture also exhibits peaks from both spectra.

Comparative protein standards (Fig. 9*A*), α-amylase (1SMD.pdb), albumin (1BM0.pdb), and hemoglobin (2DN1.pdb) proteins are used to confirm protein differences as the standards are known to differ in secondary structure and contain α/β, α, and α secondary structure, respectively. Figure 9*A* is a plot of the raw data in the form of %T versus wavenumber from 4000 to 400 cm^{-1} for α-amylase, hemoglobin, and albumin. Secondary structure was computed from the published Protein Databank files (given above). All three proteins exhibit significant stretching in the amide I region, as expected. Hemoglobin and albumin are components of blood and amylase, and α-amylase is a saliva component (2). The amylase spectrum differs significantly from the other two proteins in the 1500 to 400 cm^{-1} fingerprint region (e.g., strong 1032, 899, and 874 cm^{-1} peaks), the shape of the O–H stretch region, and a peak at 2899 cm^{-1}. The 1109 cm^{-1} peak corresponding to oxygen binding to the hemoglobin is characteristic of that protein. As predicted, they differ in the amide I region as did the body fluid samples as demonstrated by the second derivative of %T plots (Fig. 9*B*) in the 1700 to 1600 cm^{-1} regions. Additionally, the Sigma-Aldrich library IR urea spectrum (http://www.sigmaaldrich.com/labware/products/sensir-atr-library.html) was compared to that of urine, but most of the characteristic peaks are inseparable from those because of the protein although the two peaks at 3347 and 3262 cm^{-1} are faintly visible. Similarly, peaks from cholesterol, lipids, and starch were also indistinguishable from the overwhelmingly protein-like spectra. A recent publication (27) reported the use of principal component analysis to deconvolute the spectra and determine the source of each stretching or bending vibration, especially secondary structure, in proteins. Red paint and inks paint are known to have significantly different IR spectra especially in the O–H stretch and fingerprint regions as compared to proteins (19,20).

Conclusion

In this study, ATR FT-IR spectroscopy was evaluated in the detection of body fluids and materials including blood, cerumen, feces, fingernails, fingerprints, hair, nasal mucus, vaginal mucus, saliva, semen, and urine. Samples were tested in their natural liquid or solid form and as a "simulated" forensic sample by application to a square of a new, white T-shirt or white copier paper. The materials were added to a white T-shirt or white paper in a manner to simulate forensic evidence but that did not chemically alter the materials. Predictive accuracy was equally good with the appropriate air, paper, or T-shirt blank and under wet or dry conditions. Although IR spectroscopy had previously been used to examine most of these samples individually, this is the first exploration of using IR spectroscopy for presumptive testing for forensic purposes and the first presumptive test for tears and nasal mucus.

The data shown here demonstrate that ATR FT-IR spectroscopy shows promise in differentiating body fluid and materials samples using the unique peaks and stretching exhibited by the materials, especially in the fingerprint region by the unique composition of proteins but also by the presence or absence of methyl and ethyl stretches produced by lipids. In the ATR FT-spectroscopic experiments, the biological samples differ in the frequencies of the amide I peaks because of the secondary structure of the composite proteins (α or β or coil or a mixture thereof), although the C=O stretch is always present (it shifts in wavenumber depending upon the biomolecule composition). Differences are also present in the fingerprint region <1500 cm^{-1} in the raw spectra and in peak shape because of composition differences. The distinct 1016 cm^{-1} peak serves as a signature for semen, although combinations of peaks can be used to differentiate other body fluids. The lipid-containing materials (e.g., fingerprints, earwax, tears, and skin) can also be easily separated from the aqueous materials owing to the strong CH_3 asymmetric stretch of the former.

An additional study was conducted using blood and saliva to test the effect of temperature and drying; the temperatures investigated were found to have no effect on the spectra. Sample mixtures of blood and urine and blood and saliva were also investigated. The mixture spectra can be differentiated from the spectra containing only the individual samples; the new spectrum is a composite of the two components.

The use of ATR FT-IR spectroscopy for this purpose is a novel, rapid, noninvasive, nondestructive, presumptive test for body fluids and materials samples. This study demonstrates the ability of ATR FT-IR spectroscopy with access to appropriate software and library for searching and second-derivative analysis to reveal the presence of specific biological materials via a unique "fingerprint" and presumptively classify them. The method does not require preprocessing or pretreating the samples and reduces the need for expensive consumables, time-consuming presumptive tests, invasive, potentially destructive and consumptive presumptive test reagents, preserve important trace evidence and retain the integrity of the DNA for future testing. This study could be extended to include an analysis of sweat, breast milk, and sperm cells and a diverse set of substrates and environmental conditions. A database library would also need constructed prior to full field implementation.

Acknowledgments

ACS Project SEED is gratefully acknowledged for a summer stipend for Cheri Jacobs who assisted me in collecting some preliminary data during the summer of 2008. I would also like to thank two anonymous reviewers for their thoughtful review of the manuscript and helpful advice.

References

1. U.S. Department of Justice. Forensic sciences: review of status and needs. Gaithersburg, MD: AS Corporation, 1999;1–71.
2. Virkler K, Lednev IK. Analysis of body fluids for forensic purposes: from laboratory testing to non-destructive rapid confirmatory identification at a crime scene. Forensic Sci Int 2009;188(1–3):1–17.
3. Johnston E, Ames CE, Dagnall KE, Foster J, Daniel BE. Comparison of presumptive blood test kits including hexagon OBTI. J Forensic Sci 2008;53(3):687–9.
4. Tobe SS, Watson N, Nic Daeid N. Evaluation of six presumptive tests for blood, their specificity, sensitivity, and effect on high molecular-weight DNA. J Forensic Sci 2007;52(1):102–9.
5. Sidorov VL, Maiatskaia MV, Smolianitskiĭ AG, Babakhanian RV. [Establishing the presence of blood in stains for material evidence by using the luminescent blood test][Russian]. Sud Med Ekspert 1998; 41(6):20–3.
6. James SH, Nordby JJ, editors. Forensic science: an introduction to scientific and investigative techniques, 2nd edn. Boca Raton, FL: CRC Press, 2005.
7. Webb JL, Creamer JI, Quickenden TI. A comparison of the presumptive luminol test for blood with four non-chemiluminescent forensic techniques. Luminescence 2006;21(4):214–20.
8. Poon H, Elliott J, Modler J, Frégeau C. The use of Hemastix® and the subsequent lack of DNA recovery using the Promega DNA IQ™ system. J Forensic Sci 2009;54(6):1278–86.
9. Deedrick DW, Koch SL. Microscopy of hair part 1: a practical guide and manual for human hairs. Forensic Science Communications 2004 January, http://www2.fbi.gov/hq/lab/fsc/backissu/jan2004/research/2004_01_research01b.htm (accessed July 15, 2011).
10. Spear TF, Binkley SA. The HemeSelect test: a simple and sensitive forensic species test. J Forensic Sci Soc 1994;34(1):41–6.
11. Hochmeister MN, Budowle B, Sparkes R, Rudin O, Gehrig C, Thali M, et al. Validation studies of an immunochromatographic 1-step test for the forensic identification of human blood. J Forensic Sci 1999;44(3): 597–602.
12. Hochmeister MN, Budowle B, Rudin O, Gehrig C, Borer U, Thali M, et al. Evaluation of prostate-specific antigen (PSA) membrane test assays for the forensic identification of seminal fluid. J Forensic Sci 1999;44(5):1059–60.
13. Yakota M, Mitani T, Tsujita H, Kobayashi T, Higuchi T, Akane A, et al. Evaluation of a prostate-specific antigen (PSA) membrane test for forensic identification of semen. Leg Med (Tokyo) 2001;3(3):171–6.
14. Old JB, Schweers BA, Boonlayangoor PW, Reich KA. Developmental validation of RSID-saliva: a lateral flow immunochromatographic strip test for the forensic detection of saliva. J Forensic Sci 2009;54(4): 866–73.
15. Pang BC, Cheung BK. Applicability of two commercially available kits for forensic identification of saliva stains. J Forensic Sci 2008;53(5): 1117–22.
16. Myers JR, Adkins WK. Comparison of modern techniques for saliva screening. J Forensic Sci 2008;53(4):862–7.
17. Iwadate K, Doy M, Ito Y. Screening of milk aspiration in 105 infant death cases by immunostaining with anti-human alpha-lactalbumin antibody. Forensic Sci Int 2001;122(2–3):95–100.
18. Koçak A, Lucania JP, Berets SL. Some advances in fourier transform infrared transflection analysis and potential applications in forensic chemistry. Appl Spectrosc 2009;63(5):507–11.
19. Govaert F, Bernard M. Discriminating red spray paints by optical microscopy, Fourier transform infrared spectroscopy and X-ray fluorescence. Forensic Sci Int 2004;140(1):61–70.
20. Wilkinson TJ, Perry DL, Martin MC, McKinney WR, Cantu AA. Use of synchrotron reflectance infrared spectromicroscopy as a rapid, direct, nondestructive method for the study of inks on paper. Appl Spectrosc 2002;56(6):800–3.
21. Bryant CK, LaPuma PT, Hook GL, Houser EJ. Chemical agent identification by field-based attenuated total reflectance infrared detection and solid-phase microextraction. Anal Chem 2007;79(6):2334–40.
22. Kazarian SG, Chan KL. Micro- and macro-attenuated total reflection Fourier transform infrared spectroscopic imaging. Plenary Lecture at the 5th International Conference on Advanced Vibrational Spectroscopy, 2009, Melbourne, Australia. Appl Spectrosc 2010;64(5):135A–52A.

23. Lin W, Li Z. Detection and quantification of trace organic contaminants in water using the FT-IR-attenuated total reflectance technique. Anal Chem 2010;82(2):505–15.
24. Marcazzan M, Vianello F, Scarpa M, Rigo A. An ESR assay for alpha-amylase activity toward succinylated starch, amylose and amylopectin. J Biochem Biophys Methods 1999;38(3):191–202.
25. Schindler R, Lendl B, Kellner R. Simultaneous determination of α-amylase and amyloglucosidase activities using flow injection analysis with fourier transform infrared spectroscopic detection and partial least-squares data treatment. Anal Chim Acta 1998;366(1–3):35–43.
26. Imai Y, Tamaki Y. Measurement of adsorption of salivary proteins onto soft denture lining materials. J Prosthet Dent 1999;82(3):348–51.
27. Brauner JW, Flach CR, Mendelsohn R. A quantitative reconstruction of the amide I contour in the IR spectra of globular proteins: from structure to spectrum. J Am Chem Soc 2005;127(1):100–9.
28. Hall JW, Pollard A. Near-infrared spectroscopic determination of serum total proteins, albumin, globulins, and urea. Clin Biochem 1993;26(6): 483–90.
29. Dong A, Huang P, Caughey WS. Protein secondary structures in water from second-derivative amide I infrared spectra. Biochemistry 1990; 29(13):3303–8.
30. Crane NJ, Bartick EG, Perlman RS, Huffman S. Infrared spectroscopic imaging for noninvasive detection of latent fingerprints. J Forensic Sci 2007;52(1):48–53.
31. Gregoriou VG, Jayaraman V, Hu X, Spiro TG. FT-IR difference spectroscopy of hemoglobins A and Kempsey: evidence that a key quaternary interaction induces protonation of Asp beta 99. Biochemistry 1995; 34(20):6876–82.
32. Dong A, Caughey WS. Infrared methods for study of hemoglobin reaction and structures. Methods Enzymol 1994;232:139–75.
33. Thorn CE, Matcher SJ, Meglinski IV, Shore AC. Is mean blood saturation a useful marker of tissue oxygenation? Am J Physiol Heart Circ Physiol 2009;296(5):H1289–95.
34. Lyman DJ, Schofield P. Attenuated total reflection fourier transform infrared spectroscopy analysis of human hair fiber structure. Appl Spectrosc 2008;62(5):525–35.
35. Brenner L, Squires PL, Garry M, Tumosa CS. A measurement of human hair oxidation by fourier transform infrared spectroscopy. J Forensic Sci 1985;13(2):420–6.
36. Zoccola M, Aluigi A, Vineis C, Tonin C, Ferrero F, Piacentino MG. Study on cast membranes and electrospun nanofibers made from keratin/fibroin blends. Biomacromolecules 2008;9(10):2819–25.
37. Sundberg M, Peebo M, Öberg PÅ, Lundquist PG, Strömberg T. Diffuse reflectance spectroscopy of the human tympanic membrane in otitis media. Physiol Meas 2004;25(6):1473–83.
38. Cissé AS, Bluck L, Diaham B, Dossou N, Guiro AT, Wade S. Use of Fourier transformed infrared spectrophotometer (FTIR) for determination of breastmilk output by the deuterium dilution method among Senegalese women. Food Nutr Bull 2002;23(3 Suppl.):138–41.
39. Fabian H, Thi NA, Eiden M, Lasch P, Schmitt J, Naumann D. Diagnosing benign and malignant lesions in breast tissue sections by using IR-microspectroscopy. Biochim Biophys Acta 2006;1758(7):874–82.
40. Chiriboga L, Xie P, Vigorita V, Zarou D, Zakim D, Diem M. Infrared spectroscopy of human tissue. II. A comparative study of spectra of biopsies of cervical squamous epithelium and of exfoliated cervical cells. Biospectroscopy 1998;4(1):55–9.
41. Koumantakis G, Radcliff FJ. Estimating fat in feces by near-infrared reflectance spectroscopy. Clin Chem 1987;33(4):502–6.
42. Borchman D, Foulks GN, Yappert MC, Tang D, Ho DV. Spectroscopic evaluation of human tear lipids. Chem Phys Lipids 2007;147(2):87–102.
43. Nagase Y, Yoshida S, Kamiyama K. Analysis of human tear fluid by fourier transform infrared spectroscopy. Biopolymers 2005;79(1):18–27.
44. Barčot O, Balarin M, Gamulin O, Ježek D, Romac P, Brbjas-Kraljević J. Investigation of spermatozoa and seminal plasma by fourier transform infrared spectroscopy. Appl Spectrosc 2007;61(3):309–13.
45. World Medical Organization. Declaration of Helsinki. Br Med J 1996; 313(7070):1448–9.
46. Taylor EN, Curhan GC. Body size and 24-hour urine composition. Am J Kidney Dis 2006;48(6):905–15.
47. Shaw RA, Kotowich S, Mantsch HH, Leroux M. Quantitation of protein, creatinine, and urea in urine by near-infrared spectroscopy. Clin Biochem 1996;29(1):11–9.
48. Owen DH, Katz DF. A review of the physical and chemical properties of human semen and the formulation of a semen simulant. J Androl 2005;26(4):459–69.
49. Casado B, Pannell LK, Iadorola P, Baraniuk JN. Identification of human nasal mucus proteins using proteomics. Proteomics 2005;5(11):2949–59.
50. Briand L, Eloit C, Nespoulous C, Bézirard V, Huet JC, Henry C, et al. Evidence of an odorant-binding protein in the human olfactory mucus: location, structural characterization, and odorant-binding properties. Biochemistry 2002;41(23):7241–52.
51. Menefee E, Friedman M. Estimation of structural components of abnormal human hair from amino acid analyses. J Protein Chem 1985;4(5): 333–41.
52. Okuda I, Bingham B, Stoney P, Hawke M. The organic composition of earwax. J Otolaryngol 1991;20(3):212–5.
53. Burkhart CN, Burkhart CG, Williams S, Andrews PC, Adappa V, Arbogast J. In pursuit of ceruminolytic agents: a study of earwax composition. Am J Otol 2000;21(2):157–60.
54. Humphrey SP, Williamson RT. A review of saliva: normal composition, flow, and function. J Prosthet Dent 2001;85(2):162–9.

Additional information and reprint requests:
Kelly M. Elkins, Ph.D.
Director of Forensic Science
Department of Chemistry
Criminalistics Program
Metropolitan State College of Denver
PO Box 173362
Campus Box 52
Denver, CO 80217-3362
E-mail: kelkins1@mscd.edu